Light-induced synchronization modulation: enhanced in weak coupling and attenuated in strong coupling among suprachiasmatic nucleus neurons

Xu, Y.; Gu, C.G.; Qu, D.Q.; Wang, H.Y.; Rohling, J.H.T.

Light-induced synchronization modulation: Enhanced in weak coupling and attenuated in strong coupling among suprachiasmatic nucleus neurons

Yan Xu [1], Changgui Gu [1,*], Deqiang Qu [2], Haiying Wang [1], and Jos H. T. Rohling [3]

[1] *Business School, University of Shanghai for Science and Technology, Shanghai 200093, China*

[2] *School of Mathematics and Statistics, Henan University of Science and Technology, Luoyang 471023, China*

[3] *Department of Cell and Chemical Biology, Leiden University Medical Center, 2300 RC Leiden, The Netherlands*

(Received 28 June 2024; accepted 16 December 2024; published 2 January 2025)

Existing experiments demonstrated that constant light has either enhancing or diminishing effects on the behavioral rhythms of mammals, sparking our intense interest in the underlying mechanisms of this paradoxical phenomenon. The influence of constant light on behavioral rhythms involves the regulation of collective neuronal behavior. The robustness of behavioral rhythms stems from the synchronization of neurons. In mammals, the synchronization among neurons is regulated by the suprachiasmatic nucleus (SCN) located in the hypothalamus. Neurons within the SCN exhibit significant heterogeneity. The intrinsic frequency and coupling strength are two fundamental characteristics determining the internal dynamics of the SCN. In this study, the Poincaré model was employed to investigate the impact of constant light on SCN neuronal dynamics. We found that constant light can modulate neuronal synchronization, a phenomenon tightly linked to the critical threshold value of coupling strength among the neurons. Specifically, under weak coupling, constant light enhances neuronal synchronization. Under strong coupling, constant light weakens synchronization among oscillators. Furthermore, higher light intensity results in lengthened periods and reduced amplitudes. Our findings elucidate important underlying mechanisms by which constant light either enhances or diminishes mammalian behavioral rhythms, and provide a new perspective for understanding the complex regulation network of circadian rhythms.

DOI: 10.1103/PhysRevE.111.014401

I. INTRODUCTION

Constant light as a prevalent environmental condition exerts significant and intricate effects on the circadian system of mammals, particularly concerning behavioral rhythms. In previous experiments, it was observed that mice exposed to constant light exhibited either arrhythmic behavior or a low amplitude rhythm with a lengthened period, indicating that constant light can directly interfere with the daily activity patterns of mammals [1–3]. Conversely, the work of Hughes *et al.* [4] revealed that prolonged exposure to constant light in mice with VIP-VPAC2 signaling defects facilitated the restoration of behavioral rhythms close to a 24-hour period, suggesting the potential rhythm-restoring capability of constant light under specific conditions. These findings collectively underscore the dynamic regulatory role of constant light on mammalian behavioral rhythms.

The impact of constant light on the circadian rhythms of mammalian behavior involves the regulation of collective behavior of suprachiasmatic nucleus (SCN) neurons. The SCN, serving as the master clock in the mammalian brain, comprises approximately 20000 neurons [5–7]. These neurons are driven by molecular oscillators, which are part of a complex core clock-gene network. The core genes, including *mPer*, *mCry*, and *Bmal1*, form a feedback loop that regulates gene expression in a rhythmic manner [8–11]. The circadian rhythms of molecular oscillators are modulated by external light input. Specifically, light activates melanopsin-containing retinal ganglion cells, which transmit signals directly to the SCN, triggering intracellular signaling cascades, including the cAMP/CREB pathway [12,13]. At the molecular level, this signaling process regulates the transcription and translation dynamics of core clock genes, thereby altering the positive and negative feedback mechanisms within the clock-gene network [14]. At the cellular level, these molecular mechanisms lead to changes in the electrophysiological properties of SCN neurons, such as alterations in their membrane potential, firing rate, and synaptic interactions, thereby propagating information about phase and frequency to the network of neurons, leading to overall synchrony of SCN neurons [7]. These interactions in turn may manifest as shifts in the phase, frequency, and amplitude of intracellular neuronal oscillations in gene expression. The neurons in SCN are functionally heterogeneous resulting, among others, in heterogeneity in intrinsic periods, which can range from 22 to 28 hours [15]. Robust circadian rhythms are achieved through the synchronous activity of these heterogeneous neurons.

The effects of constant light on synchronization differs between healthy and unhealthy mammals. Indeed, research by Ohta *et al.* [1] found that, under constant light, the disruption of behavioral rhythms is due to the loss of synchronization among SCN neurons rather than the cessation of molecular oscillations in individual neurons. For each neuron in the SCN, constant light serves as an external perturbation that influences the expression of photoreceptive proteins, altering

*Contact author: gu_changgui@163.com

the interactions among neurons within the SCN and leading to rhythm disruption. Conversely, Hughes *et al.* [4] observed in VIP-VPAC2 signal-deficient mice that prolonged exposure to constant light improves the intercellular synchronization, thereby further enhancing the behavioral rhythmicity of animals. This finding emphasizes that the enhancement of synchronization depends on the intensity and duration of constant light. In VIP-VPAC2 signaling-deficient mice, light may promote the recovery of rhythms by activating alternative neural pathways or altering gene expression. These experiments underscore the crucial importance of synchronization in the SCN to maintain proper behavioral rhythms in organisms.

The synchronization of neurons is not only influenced by light inputs but also relies on the coupling through neurotransmitters. Neurotransmitters refer to the chemical substances that facilitate the connections and communication between neurons, playing a critical role in regulating the coupling [16,17]. Within the SCN, neurotransmitters commonly associated with coupling include vasoactive intestinal polypeptide (VIP), arginine vasopressin (AVP), γ-aminobutyric acid (GABA), gastrin-releasing peptide (GRP), among others [18]. The heterogenous neurons of the SCN achieve robust synchronization through the coupling mediated by these neurotransmitters, thereby enabling the coupled oscillator network of the SCN to generate a unified circadian rhythm [19–21]. Among these neurotransmitters, VIP is the most prevalent neuropeptide transmitter, and recent studies strongly implicate that VIP and its receptor VPAC2 play a pivotal role in the coupling of SCN cellular clocks [22,23]. For instance, research demonstrated that the application of VIP can significantly enhance coupling efficiency among SCN neurons whose coupling has been chemically disrupted [24]. In healthy mammals, the SCN structure and functionality are intact, leading to stronger coupling among neuronal oscillators within the SCN. By contrast, in mammals deficient in VIP or its receptor VPAC2, the coupling between neuronal oscillators in the SCN is notably weaker. This observation underscores the crucial impact of coupling on the synchronization among oscillators.

Constant light can either enhance or diminish the synchronization of SCN neurons; this sparked our interest, and we intend to provide a potential explanation for this paradoxical phenomenon. In this work, we utilized a coupled Poincaré model to investigate the effects of constant light on the collective behavior of strongly and weakly coupled SCN neuron ensembles. The model was detailed in Sec. II, wherein we hypothesized that intrinsic frequencies of SCN neurons are heterogeneous and follow a normal distribution around the mean. In Secs. III and IV, we presented numerical results and theoretical analyses of the impact of constant light on the synchronization, period, and amplitude of the coupled oscillator network in the SCN, respectively. Finally, we summarized and discussed our findings in Sec. V.

II. METHODS

The Poincaré model constitutes a paradigmatic exemplar of minimalistic yet comprehensive frameworks that encapsulate the fundamental attributes of oscillatory systems, specifically addressing their amplitude modulation, periodicity, phase dynamics, and stability characteristics. Notably, it was extensively employed as an analogical representation of the circadian clock mechanism, as evidenced by numerous studies such as Refs. [25–29]. This widespread adoption attests to the model's adequacy in serving as a surrogate for the investigated brain region.

In the present study, we employ a Poincaré model instantiation comprising N individual oscillators to emulate the structural and functional organization of the coupled oscillator network in the SCN. Within this model, each oscillator is mathematically represented by a bivariate system of variables, denoted as x and y. Notably, the x and y track the trajectory of the oscillating system in Cartesian space. These two variables do not directly correspond to physical concentrations of molecules but describe the oscillatory behavior in a geometric framework [30]. These oscillators are interconnected in an all-to-all manner through a mean field denoted as F, which is calculated as the arithmetic average of the x values across the entire ensemble of oscillators. In the proposed Poincaré model, the light term L is introduced to represent the effect of light input on SCN neurons. This term L can be interpreted as the mathematical representation of the biological mechanisms by which light adjusts neuronal properties, such as phase, frequency, and amplitude, which then propagate through the network and affect global synchrony. Several studies demonstrated the effectiveness of the Poincaré model in describing the interaction between light input and the circadian clock by using phase response curves [29,31–34]. Then, under the constant light, the governing equations of the Poincaré model can be formulated as follows:

$$\begin{aligned} \dot{x}_i &= \gamma x_i(A_0 - r_i) - \omega_i y_i + gF + L, \\ \dot{y}_i &= \gamma y_i(A_0 - r_i) + \omega_i x_i, \quad i = 1, 2, ..., N, \\ F &= \frac{1}{N}\sum_{i=1}^{N} x_i, \end{aligned} \tag{1}$$

where r_i, defined as $r_i = \sqrt{x_i^2 + y_i^2}$, is the actual neuronal amplitude of the ith oscillator. L is the intensity of constant light. The other parameters, such as γ, A_0, and g, represent the amplitude relaxation rate, intrinsic neuronal amplitude, and cellular coupling strength, respectively. $\omega_i = \omega_0\sigma_i$ denotes the intrinsic frequency of the ith neuron, wherein σ_i follows a normal distribution with a mean of 1 and a standard deviation of μ, $\omega_0 = \frac{2\pi}{\tau}$, τ represents the intrinsic period of neurons. We use μ to represent the heterogeneity of intrinsic frequencies for the different individual oscillators. To investigate the effects of the heterogeneity of intrinsic frequency on the synchronization, the other parameters are set as follows: $\gamma = 0.1, A_0 = 1, \tau = 24$ [29,33], and the number of neuronal oscillators is set as $N = 200$. We assume that the values of these parameters remain unchanged throughout this work if not specifically stated. Furthermore, we hypothesize that the standard deviation of intrinsic frequencies, μ, ranges from 0 to 0.2 [35,36].

We will systematically evaluate the effects of constant light on phase synchronization R, coupled period T, and amplitude r among all oscillators within the coupled oscillator network

in the SCN. R is defined as

$$R = \frac{1}{N} < \left| \sum_{j=1}^{N} e^{i\theta_j} \right| >,$$

where $\theta_j = \arctan \frac{y_j}{x_j}$ represents the phase angle of jth oscillator. The R ranges from 0 to 1. $R = 0$ indicates complete desynchronization, while $R = 1$ signifies perfect synchronization with identical phases among neurons. When oscillator j is in a stable oscillating state, the oscillation period T_j represents the time interval between consecutive peaks or troughs of variable x_j [37]. The output period T of the coupled oscillator network in the SCN is then defined as the average period across N oscillators [7], i.e.,

$$T = \frac{1}{N} \sum_{j=1}^{N} T_j.$$

Upon reaching a steady oscillatory state, the amplitude r_j of oscillator j can be computed as $r_j = \sqrt{x_j^2 + y_j^2}$ in the Poincaré model framework. Consequently, the output amplitude r of the coupled oscillator network in the SCN is defined as the average amplitude of the N oscillators, i.e.,

$$r = \frac{1}{N} \sum_{j=1}^{N} r_j.$$

In Sec. III, the fourth-order Runga-Kutta method with a time step size of 0.01 hour is performed in the numerical simulations. To avoid the effect of transients, the initial 10^5 hours are neglected. The initial values of x and y are selected randomly from a uniform distribution in the range (0, 1).

III. NUMERICAL RESULTS

In the absence of external driving, we calculate the free-running period (FRP) and phase synchronization degree R influenced by coupling strength g. FRP is defined as the average period of all coupled neuronal oscillators. We examine the relationships between FRP, R, and g under varying standard deviations μ, as depicted in Fig. 1. The categorization of coupling strength as strong or weak depends on the values of g and μ. Notably, a critical value of coupling strength g_c is labeled in Figs. 1(a)–1(c), where error bars rapidly diminish. A conspicuous change in R at g_c is observable in Fig. 1(d). When $g \geqslant g_c$, the synchronization among neural oscillators is significantly pronounced, leading us to classify the coupling strength g as strong. Conversely, if $g < g_c$, synchronization is diminished, and we term this a weak coupling strength. To illustrate, for $\mu = 0.01$, $g_c = 0.01$, $\mu = 0.05$, $g_c = 0.05$ and when $\mu = 0.10$, $g_c = 0.10$. The critical value g_c increases with the increase of intrinsic frequency heterogeneity μ. Consequently, we delineate the boundaries between strong and weak coupling strengths based on these determinations, as illustrated in Fig. 2. It is noteworthy that the distinction between strong and weak coupling strengths closely correlates with the heterogeneity of intrinsic frequencies.

Determining the strength of coupling as either strong or weak is a complex endeavor, primarily because this classification is dynamically determined by the interplay between the

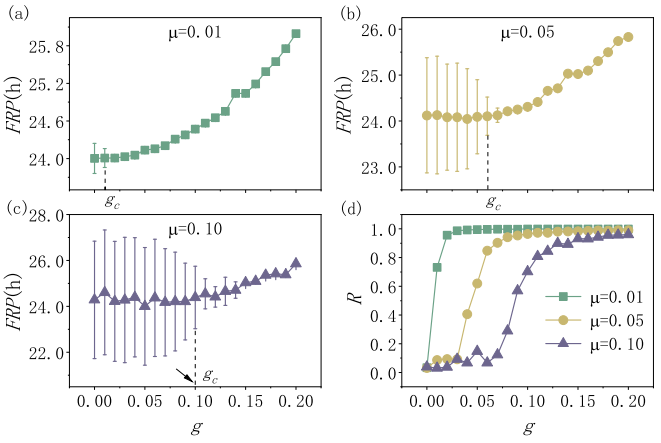

FIG. 1. The relationship of the free-running period (FRP) to the coupling strength g [panels (a)–(c)] and the relationship of R to the coupling strength g [panel (d)] in the absence of a zeitgeber ($L = 0$). The parameter μ represents the standard deviation of intrinsic neuronal frequencies, and the error bar measures the standard deviation of "coupled" neuronal periods.

value of coupling strength g and the heterogeneity of intrinsic frequencies μ. To facilitate analysis, we posit an assumption that the μ is held constant, while the g is considered variable. This assumption is considered be reasonable. Specifically, for a given biological model, such as in mice, the heterogeneity of intrinsic frequency can be viewed as an intrinsic property of the organism that is relatively stable and unchanging. Conversely, the coupling strength is more plastic and susceptible to modulation by external factors. For instance, interventions like the application of tetrodotoxin (TTX) to inhibit neural excitability or the genetic manipulation targeting genes or receptors intimately involved in coupling processes can significantly alter the coupling strength. Therefore, assuming a constant for μ while allowing g to vary not only aligns with logical coherence but also mirrors empirical observations in biological systems.

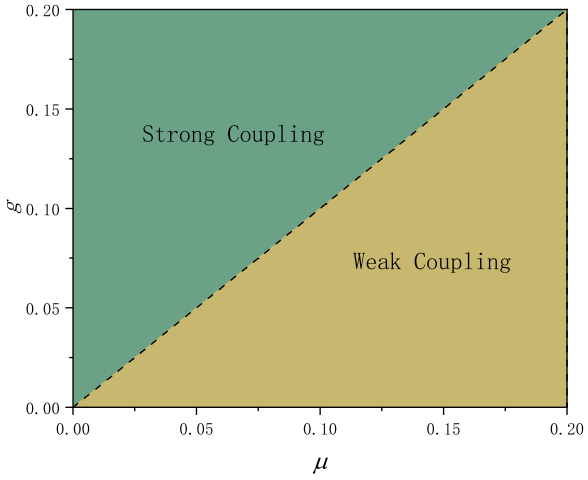

FIG. 2. The division of strong and weak coupling strengths. The dashed line represents the critical threshold g_c for strong or weak coupling strength.

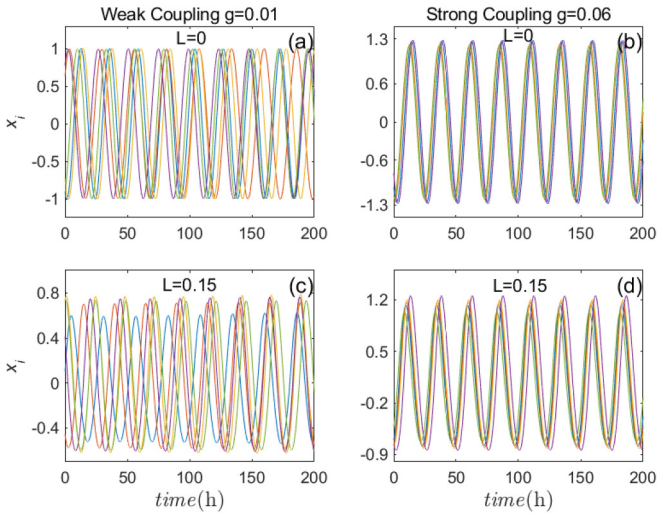

FIG. 3. The temporal evolution of five randomly selected neurons is represented by the variable x_i. Parameters g and L denote the coupling strength between neuron oscillators and the constant light intensity received, respectively. Here, the parameter selection is as follows: the heterogeneity of intrinsic frequency $\mu = 0.05$. For panels (a) and (c), the coupling strength is set to $g = 0.01$, where $L = 0$ in panel (a) and $L = 0.15$ in panel (c). For cases (b) and (d), the coupling strength is set to $g = 0.06$, where $L = 0$ in panel (b) and $L = 0.15$ in panel (d).

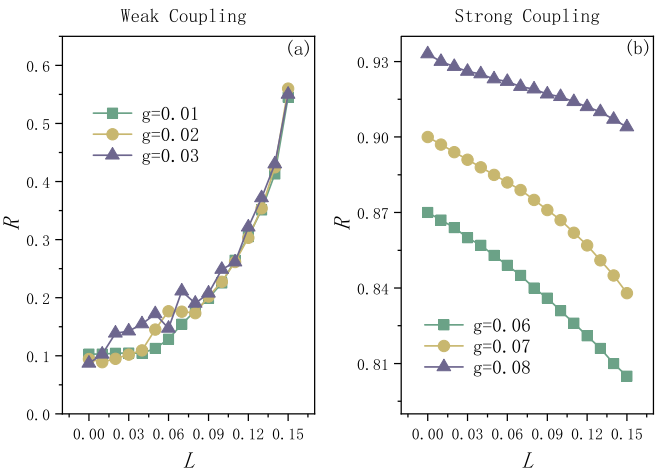

FIG. 4. The influence of constant light on the phase synchronization R of the coupled oscillator network in the SCN. Here, the heterogeneity of intrinsic frequency μ takes values of 0.05. The selected values for weak coupling strength are $g = 0.01, 0.02$, and 0.03, whereas for strong coupling strength, the representatives chosen are $g = 0.06, 0.07$, and 0.08.

A. Impact of constant light on neuronal oscillator properties: A demonstrative example

For the impact of constant light on oscillator dynamics, an illustrative example is provided in Fig. 3, considering a fixed intrinsic frequency. It becomes heterogeneous with a standard deviation of $\mu = 0.05$, which was often used previously [38–40]. Based on Fig. 2, it is evident that when $\mu = 0.05$, $g = 0.01$ represents weak coupling strength, while $g = 0.06$ represents strong coupling strength. The $\mathrm{VIP}^{-/-}$ knock-out mice, which lack VIP expression, exhibit disturbed coupling, and this is modeled by weakening the coupling strength, whereas healthy animals, with normal VIP expression, have stronger coupling strength. In Fig. 3, weak coupling strength refers to the $\mathrm{VIP}^{-/-}$ animals, while strong coupling strength corresponds to the healthy animals.

When the oscillators are in constant darkness ($L = 0$), the temporal evolution of the neuronal ensemble exhibits similar amplitudes but erratic phase behavior under weak coupling strength ($g = 0.01$), indicative of substantial phase disparities and thus poor synchronization among the oscillators, as demonstrated in Fig. 3(a). Conversely, as observed in Fig. 3(b), under strong coupling strength ($g = 0.06$), the oscillators demonstrate ordered behavior, indicating well synchronization among them, oscillating with consistent periods and amplitudes.

Upon introducing constant light with intensity $L = 0.15$, the temporal evolution of the neural population under weak coupling exhibits a more regular pattern, although not all oscillators synchronize, implying that constant light can improve the synchronization among weakly coupled oscillators, as illustrated in Fig. 3(c), reflecting the experimental results from Ref. [4]. It should be noted, however, that not all oscillators maintain a uniform period, and amplitudes significantly decrease. In stark contrast, constant light induces slight perturbations in the temporal evolution of strongly coupled neuronal populations, with synchronization between oscillators showing a decrease compared to constant darkness. This indicates a desynchronizing effect of constant light on strongly coupled oscillators, as evident in Fig. 3(d), reflecting the experimental results from Ref. [1]. These modeling results indicate that the model described here is able to explain mechanistically the differential effects of constant light seen in experiments.

Subsequently, we shall systematically investigate the effects of constant light on the phase synchronization, periods, and amplitudes of the neural population.

B. Effects of constant light on neuronal oscillator synchronization under strong and weak coupling

The diverse impacts of constant light on neuronal oscillator synchronization degree R are vividly illustrated in Fig. 4. Here we select a fixed frequency heterogeneity of $\mu = 0.05$. Therefore, according to Fig. 2, we can determine the critical value $g_c = 0.05$ that distinguishes strong and weak coupling.

Observations from Fig. 4 reveal dual effects of constant light on the synchronization of the coupled oscillator network in the SCN. Specifically, under weak coupling strength, i.e., $g < g_c$, constant light enhances the synchronization among neurons, as shown in Fig. 4(a). Particularly, the enhancement of constant light on synchronization is slight and unstable when the light intensity $L < 0.08$. However, at $L \geqslant 0.08$, the synchronization of coupled oscillator network in the SCN is enhanced robustly and swiftly by constant light. Under strong coupling strength, i.e., $g \geqslant g_c$, we observe that constant light exhibits desynchronizing effects on synchronization R, as depicted in Fig. 4(b). Notably, the synchronization decreases most noticeably at $g = 0.06$, while the decrease is minimal at $g = 0.08$. This indicates that the synchronization of the

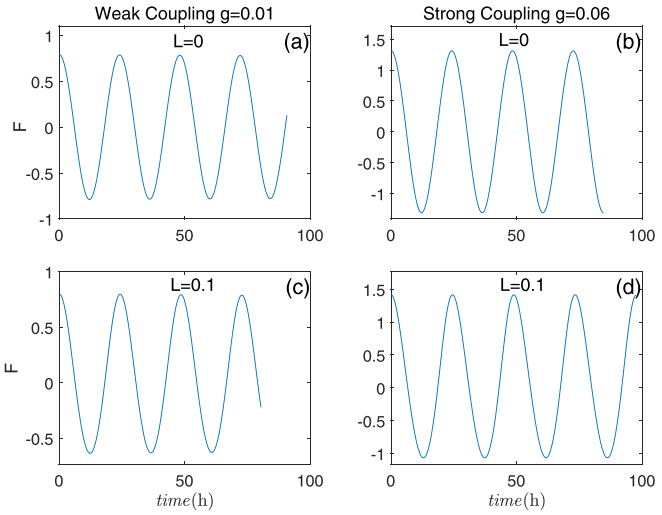

FIG. 5. Temporal dynamics of the mean field under varying light intensities in weak and strong coupling regimes. The number of oscillators is $N = 200$ and the heterogeneity of intrinsic frequency μ takes values of 0.05. The selected value for weak coupling strength is $g = 0.01$, whereas for strong coupling strength $g = 0.06$.

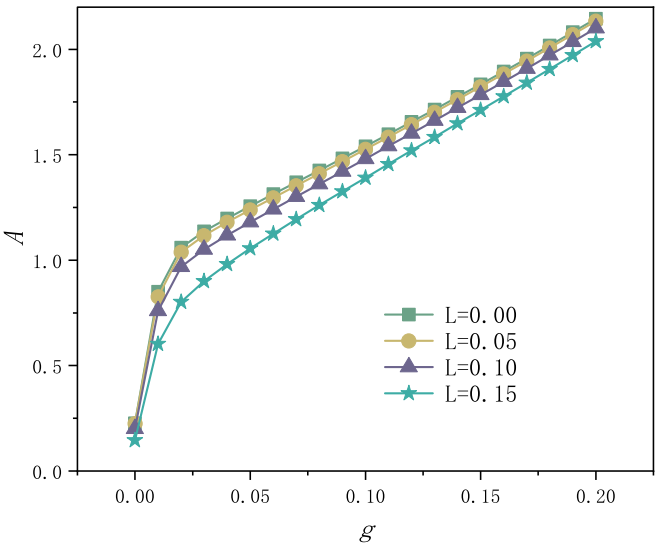

FIG. 6. The relationship between the amplitude A of the mean field F and the coupling strength g under different intensities of constant light.

coupled oscillator network in the SCN is more susceptible to disruption by constant light when the coupling strength between neuronal oscillators is lower.

In the Poincaré model, the dynamics of each neuron are described by three main components,

$$\dot{x}_i = h(x_i, y_i) + gF + L, \tag{2}$$

where $h(x_i, y_i)$ represents the intrinsic dynamics of the neuron, gF is the coupling term reflecting the influence of the network, and L is the light input acting as an external force. These three components jointly determine the behavior of each neuron and the overall synchronization of the network.

An important point to note is that the mean filed $F = \frac{1}{N}\sum_{j=1}^{N} x_j$ is a time-varying variable, as shown in Fig. 5, which means that it oscillates over time as the network evolves. Therefore, instead of analyzing F directly, we focus on the amplitude of F, denoted as A. The amplitude A captures the oscillatory behavior of F and provides a more stable measure for examining the collective dynamics. As shown in Fig. 6, A is proportional to the coupling strength g, allowing us to reliably substitute A for F when investigating the dynamics of the system.

These observations in Fig. 4 naturally lead to an important consideration regarding the balance between the coupling term gF and the light input L in regulating the synchronization dynamics. To quantitatively analyze the relative influence of the coupling term and the light input, we introduce the ratio gA/L, where A represents the amplitude of the mean field F. This ratio helps capture the interplay between the coupling and the light input across different coupling strengths and light intensities. As shown in Fig. 7, the plot of gA/L as a function of L reveals critical insights. For weak coupling $g = 0.01$, gA/L is consistently less than 1, indicating that the light input L dominates and promotes synchronization. On the other hand, for strong coupling $g = 0.15$, gA/L exceeds 1, showing that the coupling term gF takes the lead in dictating the dynamics, with the light input instead disrupting the synchronization.

C. Effects of constant light on SCN period under strong and weak coupling

The impact of constant light on the coupled period T is investigated, with the heterogeneity $\mu = 0.05$ of intrinsic frequency, then the coupling strength g from 0 to 0.05 is the weak coupling strength and g from 0.05 to 0.20 is the strong coupling strength, as depicted in Fig. 8.

Under both strong and weak coupling conditions, the influence of constant light intensity on the coupled period T is similar. Specifically, when the coupling strength g is set to a fixed value, the period of the coupled oscillator network in the

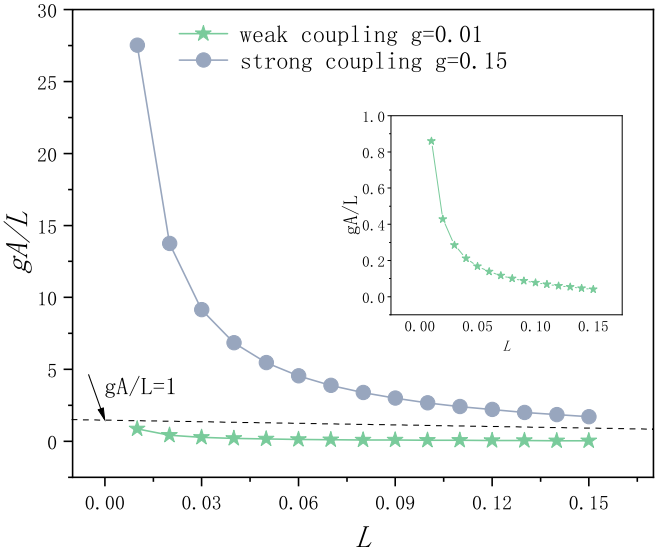

FIG. 7. Ratio of gA/L as a function of L for weak coupling $g = 0.01$ and strong coupling $g = 0.15$.

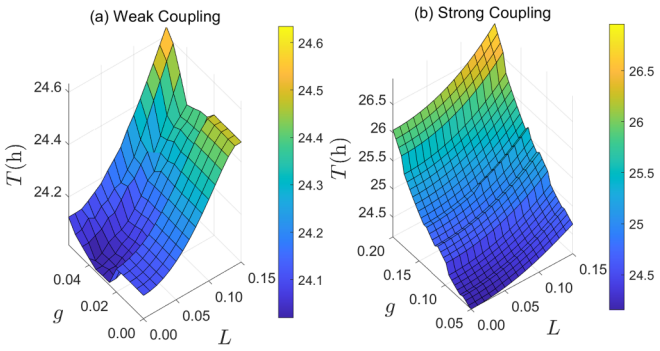

FIG. 8. The comprehensive impact of constant light and coupling strength on the period of coupled oscillator network in the SCN. The heterogeneity μ of intrinsic frequency is selected as 0.05.

SCN increases monotonically with increasing constant light intensity, and is not affected by the coupling strength critical value g_c. Additionally, when the constant light intensity L is set to a fixed value, the period of the coupled oscillator network in the SCN increases with increasing coupling strength, as shown in Figs. 8(a) and 8(b), consistent with the effect of coupling strength on the oscillation period under constant darkness in Figs. 1(a)–1(c). We also observe that under weak coupling strength, the coupled period T is generally smaller than under strong coupling strength.

D. Effect of constant light on SCN amplitude under strong and weak coupling

Constant light exerts a negative impact on the amplitude of the coupled oscillator network in the SCN, as illustrated in Figs. 9(a) and 9(b). When the coupling strength g is held constant, the amplitude decreases with increasing constant light intensity, irrespective of the critical value of coupling strength g_c. SCN-coupled oscillator networks under weak coupling are more susceptible to constant light, with amplitudes decreasing from approximately 1 to around 0.6. The decline in amplitude is more pronounced with lower coupling strengths. In contrast, under strong coupling strength, the interference of constant light on the coupled oscillator network in the SCN amplitudes is less significant, and the trend of amplitude reduction becomes more subtle as coupling strength increases. When constant light intensity L is fixed, the amplitude of the coupled oscillator network in

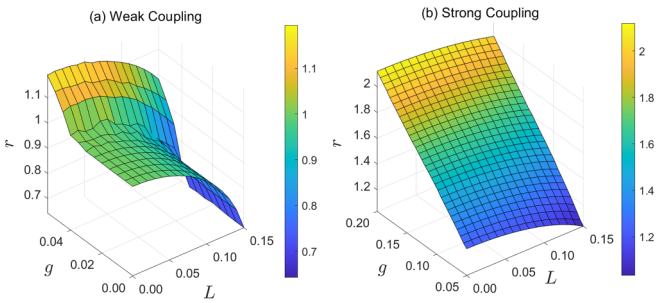

FIG. 9. The comprehensive impact of constant light and coupling strength on the amplitude of coupled oscillator network in the SCN. The heterogeneity μ of intrinsic frequency is selected as 0.05.

the SCN increases with higher coupling strength. Comparing (a) with (b) in Fig. 9, it is evident that SCN amplitudes under strong coupling are notably larger than those under weak coupling.

An all-to-all coupled network is often used as a global approximation to the many synaptic interactions between the cells in the SCN. A more realistic approach would mean to take into account the network topology, i.e., the scheme that tells which neurons are connected to which other neurons. Currently this information is unknown. Apart from this, the network connections are also not static. The connectivity in the network is constantly changing: connections are created or are broken, connections get stronger or weaker over time. To approximate the network, many studies use the global all-to-all coupling scheme [15,29,39,41]. There are also studies that investigate different possible network topologies [42–47]. But also for these studies, one can not claim to simulate the "real" system, as the "real" network topology is unknown. However, to address this topic, we conduct a detailed examination of the effects of two heterogeneous networks on synchronization dynamics: an Erdös-Rényi (ER) random network [48], which represents low heterogeneity, and a Barabási-Albert (BA) scale-free network [49], indicative of high heterogeneity. The results are qualitatively consistent with those shown in Figs. 4, 8, and 9. Detailed description of model with heterogeneous coupling and corresponding results, Figs. S1–S3, are presented in the Supplementary Material [50]. To facilitate theoretical analysis, we employed an all-to-all network model in Sec. IV.

Additionally, we conduct an examination of the synchronization dynamics in systems with oscillator number $N = 1000$ and $N = 10\,000$. The findings indicate that the synchronization dynamics remain unaffected even with a substantial increase in the number of oscillators. Detailed result Fig. S4 is presented in the Supplementary Material [50]. This observation underscores the robustness of our results, demonstrating their broad applicability to large-scale systems.

IV. ANALYTICAL RESULTS

In this section, analytical results are provided to explain the emergence of positive relationship between coupling strength and critical value of heterogeneity, the increasing effect of constant light on the period, and the decreasing effect of constant light on the amplitude, respectively. To simplify the analysis, let the number of neuron oscillator be $N = 2$. Equation (1) can be rewritten as

$$\begin{aligned}
\dot{x_1} &= \gamma x_1(A_0 - r_1) - \omega_1 y_1 + g\frac{x_1 + x_2}{2} + L,\\
\dot{y_1} &= \gamma y_1(A_0 - r_1) + \omega_1 x_1,\\
\dot{x_2} &= \gamma x_2(A_0 - r_2) - \omega_2 y_2 + g\frac{x_1 + x_2}{2} + L,\\
\dot{y_2} &= \gamma y_2(A_0 - r_2) + \omega_2 x_2.
\end{aligned} \tag{3}$$

For convenience, Eq. (3) is transformed from Cartesian coordinates to polar coordinates. Suppose $x_1 = r_1\cos\theta_1$, $y_1 = r_1\sin\theta_1$, $x_2 = r_2\cos\theta_2$, $y_2 = r_2\sin\theta_2$, substituting them into

Eq. (3) and we obtain

$$\begin{aligned}
\dot{r_1} &= \gamma r_1(A_0 - r_1) + \frac{r_1\cos^2\theta_1 + r_2\cos\theta_1\cos\theta_2}{2}g \\
&\quad + L\cos\theta_1, \\
\dot{\theta_1} &= \omega_1 - \frac{r_1\sin\theta_1\cos\theta_1 + r_2\sin\theta_1\cos\theta_2}{2r_1}g - \frac{L\sin\theta_1}{r_1}, \\
\dot{r_2} &= \gamma r_2(A_0 - r_2) + \frac{r_2\cos^2\theta_2 + r_1\cos\theta_1\cos\theta_2}{2}g \\
&\quad + L\cos\theta_2, \\
\dot{\theta_2} &= \omega_2 - \frac{r_1\sin\theta_2\cos\theta_1 + r_2\sin\theta_2\cos\theta_2}{2r_2}g - \frac{L\sin\theta_2}{r_2}. \quad (4)
\end{aligned}$$

When the frequencies of these two oscillators are the same (locked), we have $\dot{r_1} = 0, \dot{r_2} = 0, \dot{\theta_1} = \Omega, \dot{\theta_2} = \Omega$, where Ω is the coupled frequency of these two oscillators. Consequently, we let $\theta_1 = \Omega t + \phi_1$, $\theta_2 = \Omega t + \phi_2$. Considering the averaging method developed by Krylov and Bogoliubov as used in Refs. [29,51], suppose $\alpha = \theta_2 - \theta_1$, then we have

$$\begin{aligned}
&< \cos^2(\phi_1 + \Omega t) > = \frac{1}{2}, \\
&< \cos(\phi_2 + \Omega t)\cos(\phi_1 + \Omega t) > = \frac{\cos(\phi_1 - \phi_2)}{2} \equiv \frac{\cos\alpha}{2}, \\
&< \cos(\phi_1 + \Omega t)\sin(\phi_1 + \Omega t) > = 0, \\
&< \cos(\phi_2 + \Omega t)\sin(\phi_1 + \Omega t) > = -\frac{\sin\alpha}{2}, \\
&< \cos(\phi_1 + \Omega t)\sin(\phi_2 + \Omega t) > = \frac{\sin\alpha}{2}, \quad (5)
\end{aligned}$$

where $< \cdot >$ denotes the average in one cycle. For simplicity, we keep on the nonaverage notation r_1, r_2, ϕ_1, and ϕ_2 in the following. Substituting Eq. (5) into Eq. (4), we get

$$\begin{aligned}
0 &= \gamma r_1(A_0 - r_1) + \frac{(r_1 + r_2\cos\alpha)g}{4} + L\cos\theta_1, \\
\Omega &= \omega_1 + \frac{r_2 g\sin\alpha}{4r_1} - \frac{L\sin\theta_1}{r_1}, \\
0 &= \gamma r_2(A_0 - r_2) + \frac{(r_1\cos\alpha + r_2)g}{4} + L\cos\theta_2, \\
\Omega &= \omega_2 - \frac{r_1 g\sin\alpha}{4r_2} - \frac{L\sin\theta_2}{r_2}. \quad (6)
\end{aligned}$$

From Eq .(6) we have that

$$\begin{aligned}
\cos\theta_1 &= \frac{\gamma r_1(A_0 - r_1) + (r_1 + r_2\cos\alpha)\frac{g}{4}}{-L}, \\
\sin\theta_1 &= \frac{r_1\left(\omega_1 - \Omega + \frac{r_2 g\sin\alpha}{4r_1}\right)}{L}, \\
\cos\theta_2 &= \frac{\gamma r_2(A_0 - r_2) + (r_2 + r_1\cos\alpha)\frac{g}{4}}{-L}, \\
\sin\theta_2 &= \frac{r_2\left(\omega_2 - \Omega + \frac{r_1 g\sin\alpha}{4r_2}\right)}{L}. \quad (7)
\end{aligned}$$

By $\sin^2\theta_1 + \cos^2\theta_1 = 1$, $\sin^2\theta_2 + \cos^2\theta_2 = 1$, and when the oscillators are synchronized, the amplitudes of these two oscillators are almost equal, i.e., $r \equiv r_1 \approx r_2 \approx 1$ [as shown in Fig. 3(b)], Eq. (7) can be reduced as

$$\begin{aligned}
&\left[\gamma r(A_0 - r) + r(1 + \cos\alpha)\frac{g}{4}\right]^2 \\
&\quad + \left[r\left(\omega_1 - \Omega + \frac{g\sin\alpha}{4}\right)\right]^2 = L^2, \\
&\left[\gamma r(A_0 - r) + r(1 + \cos\alpha)\frac{g}{4}\right]^2 \\
&\quad + \left[r\left(\omega_2 - \Omega - \frac{g\sin\alpha}{4}\right)\right]^2 = L^2. \quad (8)
\end{aligned}$$

The addition of the two equations of Eq. (8) yields

$$\begin{aligned}
&\left[\left(\omega_1 - \Omega + \frac{g\sin\alpha}{4}\right) + \left(\omega_2 - \Omega - \frac{g\sin\alpha}{4}\right)\right]^2 \\
&\quad + 2\left[\gamma(A_0 - r) + (1 + \cos\alpha)\frac{g}{4}\right]^2 = \frac{2L^2}{r^2}. \quad (9)
\end{aligned}$$

When the oscillators are synchronized, the phase difference $\alpha \to 0$, then there is $\cos\alpha \to 1$ and $\sin\alpha \to 0$. We set $\omega_1 = \omega_0(1 - \mu)$ and $\omega_2 = \omega_0(1 + \mu)$, thus the Eq. (9) can be simplified as

$$(\omega_0 - \Omega)^2 + Q = \tfrac{L^2}{r^2}, \quad (10)$$

where $Q = \omega_0^2\mu^2 + \frac{g^2}{4} + \gamma(A_0 - r)g + \gamma^2(A_0 - r)^2$. Since the period $T > 24$ hours when the oscillator remains synchronized, therefore $\Omega < \omega_0$, then we can obtain the coupled frequency Ω from Eq. (10), i.e.,

$$\Omega \approx \omega_0 - \sqrt{\tfrac{L^2}{r^2} - Q}, \quad (11)$$

this indicates that the coupling frequency Ω is negatively correlated with the constant light intensity, from which it can be inferred that the coupled period T is positively correlated with the constant light intensity L, which qualitatively explains the relationship between the T and the L in Fig. 5.

When the oscillators are synchronized, the amplitude r of the oscillators is approximately equal to 1. Then from Eq. (10) we have

$$\begin{aligned}
&(\omega_0 - \Omega)^2 + \omega_0^2\mu^2 + \frac{g^2}{4} + \gamma(A_0 - r)g \\
&\quad + \gamma^2\left(A_0^2 - 2rA_0 + 1\right) \approx L^2, \quad (12)
\end{aligned}$$

thus the amplitude is

$$r \approx \frac{-L^2}{\gamma(2\gamma A_0 + g)} + \frac{M}{\gamma(2\gamma A_0 + g)}, \quad (13)$$

where $\gamma(2\gamma A_0 + g) > 0$ and $M = \gamma^2(A_0^2 + 1) + \gamma g A_0 + \frac{g^2}{4} + (\omega_0 - \Omega)^2 + \omega_0^2\mu^2 > 0$. This indicates that the amplitude r decreases as the constant light intensity L increases, which is qualitatively consistent with Fig. 6.

From Fig. 3, we see that when the oscillators are synchronized, there exists $g \geqslant g_c$, hence subtracting the two expressions of Eq. (8), we can obtain

$$\left(\omega_1 - \Omega + \frac{g_c\sin\alpha}{4}\right)^2 - \left(\omega_2 - \Omega - \frac{g_c\sin\alpha}{4}\right)^2 = 0, \quad (14)$$

that is

$$(\omega_1 + \omega_2 - 2\Omega)\left(\omega_1 - \omega_2 + \tfrac{g_c \sin\alpha}{2}\right) = 0. \tag{15}$$

Then we get

$$g_c = \tfrac{4\mu\omega_0}{\sin\alpha}, \tag{16}$$

since $\omega_1 + \omega_2 - 2\Omega \neq 0$. This qualitatively indicates that the critical threshold value g_c of coupling strength is positively correlated with the intrinsic frequency heterogeneity μ, as shown by the dashed line in Fig. 2.

V. CONCLUSIONS AND DISCUSSION

In the present study, we examined the varied effects of constant light on the entrainment of the SCN that were found experimentally, by looking at the synchronization, period, and amplitude of the SCN neuronal network, based on a generalized Poincaré model containing neurons with intrinsic frequency heterogeneity. Employing numerical simulations and theoretical analyses, we elucidated the dual regulatory mechanism of constant light on the synchronization effects among neuronal oscillators, which is closely linked to a critical threshold value of coupling strength. Specifically, (i) in the case of weak coupling, i.e., when the coupling strength is below the critical value, constant light exhibits a facilitative role and enhances synchronization among neurons. Conversely, (ii) under strong coupling strength, i.e., when the coupling strength is larger than the critical value, constant light weakens the synchronization among neuronal oscillators. Furthermore, we determined that there is a linear positive correlation between the critical value of coupling strength and intrinsic frequency heterogeneity. This implies that the critical value of the coupling strength increases linearly with the increase of the intrinsic frequency heterogeneity. The effect of constant light on the period and amplitude is relatively simple: as the constant light intensity increases, the period of the SCN increases and the amplitude decreases.

Constant light, serving as a persistent and unvarying zeitgeber, was gradually recognized by the scientific community as a lighting condition potentially compromising the integrity and normal physiological functioning of biological organisms. Indeed, it was documented that constant light exposure disrupts the behavioral rhythms in healthy mammals [1]. We speculated that this phenomenon is related to a critical threshold value of coupling strength. Specifically, when the coupling strength between neuronal oscillators is strong, and this coupling strength does not exceed a critical threshold related to intrinsic frequency heterogeneity, then their ability to recover from constant light interference is diminished. This leads to a reduction in synchronization and thus to arrhythmic behavior.

However, constant light shows therapeutic potential for animals with severely disrupted circadian rhythm systems. Researches confirmed that VIP and its VPAC2 receptors play a central role in the cellular signaling network within the SCN, being crucial for mediating intercellular synchronization [7,22,52]. When intracellular clock mechanisms or intercellular neuropeptide signaling pathways involving the VIP-VPAC2 pathway are impaired, the coupling strength among SCN neurons is significantly weakened. Studies indicated that constant light exposure can alleviate the impact of impaired intercellular signaling on SCN neurons, aiding in restoring disrupted behavioral rhythms [4]. We inferred that constant light plays an active role when the coupling strength between neuronal oscillators is weak, and this coupling strength does not exceed a critical threshold related to intrinsic frequency heterogeneity. The coupled oscillator network in the SCN responds to the light input by altering the phase distribution of heterogeneous neurons. This alteration enhances the synchronization between the oscillators, thereby further enhancing behavioral rhythmicity.

Under the condition of constant light, the phenomenon of elongated behavioral circadian period accompanied by decreased amplitude in animals may be associated with the process of light adaptation within organisms. Light signals serve as a primary input to the circadian clock, and sustained exposure to light may lead to a gradual reduction in the organism's responsiveness to such signals. Consequently, the circadian clock may require an extended period to synchronize its internal rhythms with the external environment, thus resulting in a lengthened behavioral circadian period. An explanation of this amplitude reduction is given as phase dispersion among rhythmic SCN cells [18]. In particular, under constant light, the amplitude reduction in wild-type mice is significantly more pronounced compared to that in VIP-deficient mice, thereby robustly corroborating the consistency between our findings and the experimental data presented in Ref. [53] concerning amplitude variations.

The findings presented herein not only deepen our understanding of the mechanisms by which the light influences the regulation of biological rhythms but also provide a new perspective and theoretical foundation for exploring prevention mitigation strategies for health issues, such as circadian disruptions and sleep disorders, induced by abnormal light exposures.

Coupling plays an essential role in maintaining the robustness of circadian rhythms. It was found that the nonidentical neurons are well synchronized through the coupling of chemical neurotransmitters, such as VIP, AVP, GABA, in that the neurons show a uniform circadian period [19–21,52]. Nevertheless, the neural system responses to constant light is complex, possibly involving some form of sensory adaptation and an impact on neuron coupling. In previous models, coupling strength was often assumed to be constant and averaged, which may be too rigid a view. For complex biological systems with synchronous dynamics, it is more reasonable to adjust coupling strength based on the proximity of initial and synchronous states [54,55]. Therefore, in future works, we plan to introduce adaptive coupling strength to challenge the constant coupling strength assumption in the model and make it closer to real-world conditions.

ACKNOWLEDGMENTS

This work is supported by the National Natural Science Foundation of China under Grants No. 12275179 and No. 12305047 and Natural Science Foundation of Shanghai, China (Grant No. 21ZR1443900). This work is supported by High Performance Computing Center, University of Shanghai for Science and Technology.

[1] H. Ohta, S. Yamazaki, and D. G. McMahon, Constant light desynchronizes mammalian clock neurons, Nat. Neurosci. **8**, 267 (2005).

[2] C. S. Pittendrigh and S. Daan, A functional analysis of circadian pacemakers in nocturnal rodents, J. Comp. Physiol. **106**, 223 (1976).

[3] T. Moriya, Y. Yoshinobu, Y. Kouzu, A. Katoh, H. Gomi, M. Ikeda, T. Yoshioka, S. Itohara, and S. Shibata, Involvement of glial fibrillary acidic protein (GFAP) expressed in astroglial cells in circadian rhythm under constant lighting conditions in mice, J. Neurosci. Res. **60**, 212 (2000).

[4] A. T. L. Hughes, C. L. Croft, R. E. Samuels, T. Takumi, and H. D. Piggins, Constant light enhances synchrony among circadian clock cells and promotes behavioral rhythms in VPAC2-signaling deficient mice, Sci. Rep. **5**, 14044 (2015).

[5] D. A. Golombek and R. E. Rosenstein, Physiology of circadian entrainment, Physiol. Rev. **90**, 1063 (2010).

[6] D. C. Klein, R. Y. Moore, and S. M. Reppert, *Suprachiasmatic Nucleus: The Mind's Clock* (Oxford University Press, New York, 1991).

[7] D. K. Welsh, J. S. Takahashi, and S. A. Kay, Suprachiasmatic nucleus: Cell autonomy and network properties, Annu. Rev. Physiol. **72**, 551 (2010).

[8] J. S. Takahashi, Transcriptional architecture of the mammalian circadian clock, Nat. Rev. Genet. **18**, 164 (2017).

[9] S. M. Reppert and D. R. Weaver, Molecular analysis of mammalian circadian rhythms, Annu. Rev. Physiol. **63**, 647 (2001).

[10] L. P. Shearman, S. Sriram, D. R. Weaver, E. S. Maywood, I. Chaves, B. Zheng, K. Kume, C. C. Lee, G. T. J. van der, Horst, M. H. Hastings, and S. M. Reppert, Interacting molecular loops in the mammalian circadian clock, Science **288**, 1013 (2000).

[11] S. M. Reppert and D. R. Weaver, Coordination of circadian timing in mammals, Nature (London) **418**, 935 (2002).

[12] T. M. Schmidt, M. T. H. Do, D. Dacey, R. Lucas, S. Hattar, A. Matynia, Melanopsin-positive intrinsically photosensitive retinal ganglion cells: From form to function, J. Neurosci. **31**, 16094 (2011).

[13] M. H. Berry, M. Moldavan, T. Garrett, M. Meadows, O. Cravetchi, E. White, J. Leffler, H. von Gersdorff, K. M. Wright, C. N. Allen, and B. Sivyer, A melanopsin ganglion cell subtype forms a dorsal retinal mosaic projecting to the supraoptic nucleus, Nat. Commun. **14**, 1492 (2023).

[14] F. Fagiani, D. Di Marino, A. Romagnoli, C. Travelli, D. Voltan, L. Di Cesare Mannelli, M. Racchi, S. Govoni, and C. Lanni, Molecular regulations of circadian rhythm and implications for physiology and diseases, Sig. Transduct. Target Ther. **7**, 41 (2022).

[15] C. Gu, J. Wang, and Z. Liu, Free-running period of neurons in the suprachiasmatic nucleus: Its dependence on the distribution of neuronal coupling strengths, Phys. Rev. E **80**, 030904(R) (2009).

[16] J. A. Mohawk and J. S. Takahashi, Cell autonomy and synchrony of suprachiasmatic nucleus circadian oscillators, Trends Neurosci. **34**, 349 (2011).

[17] S. J. Aton, J. E. Huettner, M. Straume, and E. D. Herzog, GABA and $G_{i/o}$ differentially control circadian rhythms and synchrony in clock neurons, Proc. Natl. Acad. Sci. USA **103**, 19188 (2006).

[18] A. Ramkisoensing and J. H. Meijer, Synchronization of biological clock neurons by light and peripheral feedback systems promotes circadian rhythms and health, Front. Neurol. **6**, 128 (2015).

[19] H. Albus, M. J. Vansteensel, S. Michel, G. D. Block, and J. H. Meijer, A GABAergic mechanism is necessary for coupling dissociable ventral and dorsal regional oscillators within the circadian clock, Curr. Biol. **15**, 886 (2005).

[20] A. B. Webb, N. Angelo, J. E. Huettner, and E. D. Herzog, Intrinsic, nondeterministic circadian rhythm generation in identified mammalian neurons, Proc. Natl. Acad. Sci. USA **106**, 16493 (2009).

[21] I. T. Tokuda, D. Ono, B. Ananthasubramaniam, S. Honma, K. Honma, and H. Herzel, Coupling controls the synchrony of clock cells in development and knockouts, Biophys. J. **109**, 2159 (2015).

[22] E. S. Maywood, A. B. Reddy, G. K. Y. Wong, J. S. O'Neill, J. A. O'Brien, D. G. McMahon, A. J. Harmar, H. Okamura, and M. H. Hastings, Synchronization and maintenance of timekeeping in suprachiasmatic circadian clock cells by neuropeptidergic signaling, Curr. Biol. **16**, 599 (2006).

[23] A. T. L. Hughes, C. Guilding, L. Lennox, R. E. Samuels, D. G. McMahon, and H. D. Piggins, Live imaging of altered *period1* expression in the suprachiasmatic nuclei of $Vipr2^{-/-}$ mice, J. Neurochem. **106**, 1646 (2008).

[24] M. H. Wang, N. Chen, and J. H. Wang, The coupling features of electrical synapses modulate neuronal synchrony in hypothalamic superachiasmatic nucleus, Brain Res. **1550**, 9 (2014).

[25] L. Glass and M. C. Mackey, *From Clocks to Chaos: The Rhythms of Life* (Princeton University Press, Princeton, NJ, 1988).

[26] C. Schmal, H. Herzel, and J. Myung, Clocks in the wild: Entrainment to natural light, Front. Physiol. **11**, 272 (2020).

[27] C. G. Gu, H. J. Yang, M. Wang, and J. H. T. Rohling, Heterogeneity in relaxation rate improves the synchronization of oscillatory neurons in a model of the SCN, Chaos **29**, 013103 (2019).

[28] C. Schmal, J. Myung, H. Herzel, and G. Bordyugov, A theoretical study on seasonality, Front. Neurol. **6**, 94 (2015).

[29] U. Abraham, A. E. Granada, P. O. Westermark, M. Heine, A. Kramer, and H. Herzel, Coupling governs entrainment range of circadian clocks, Mol. Syst. Biol. **6**, 438 (2010).

[30] D. Olmo, S. Grabe, H. Herzel, Mathematical modeling in circadian rhythmicity, Methods Mol. Biol. **2482**, 55 (2022).

[31] A. Granada, R. M. Hennig, B. Ronacher, A. Kramer, H. Herzel, Phase response curves: Elucidating the dynamics of coupled oscillators, Methods Enzymol.: Comput. Methods **454**, 1 (2009).

[32] G. B. Ermentrout, L. Glass, B. E. Oldeman, The shape of phase-resetting curves in oscillators with a saddle node on an invariant circle bifurcation, Neural Comput. **24**, 3111 (2012).

[33] C. G. Gu, H. J. Yang, J. H. Meijer, and J. H. T. Rohling, Dependence of the entrainment on the ratio of amplitudes between two subgroups in the suprachiasmatic nucleus, Phys. Rev. E **97**, 062215 (2018).

[34] T. Krogh-Madsen, R. Butera, G. B. Ermentrout, and L. Glass, Phase Resetting Neural Oscillators: Topological Theory Versus the Realworld, in *Phase Response Curves in Neuroscience: Theory, Experiment, and Analysis* (Springer-Verlag, New York, 2012), pp. 33–51.

[35] C. G. Gu, J. S. Xu, Z. H. Liu, and J. H. T. Rohling, Entrainment range of nonidentical circadian oscillators by a light-dark cycle, Phys. Rev. E **88**, 022702 (2013).

[36] I. M. Usmani, D. J. Dijk, and A. C. Skeldon, Mathematical analysis of light-sensitivity related challenges in assessment of the intrinsic period of the human circadian pacemaker, J. Biol. Rhythms **39**, 166 (2024).

[37] D. Gonze, Modelling circadian clocks: From equations to oscillations, Open Life Sci. **6**, 699 (2011).

[38] C. G. Gu, J. H. T. Rohling, X. M. Liang, and H. J. Yang, Impact of dispersed coupling strength on the free running periods of circadian rhythms, Phys. Rev. E **93**, 032414 (2016).

[39] J. C. W. Locke, P. O. Westermark, A. Kramer, and H. Herzel, Global parameter search reveals design principles of the mammalian circadian clock, BMC Syst. Biol. **22**, 2 (2008).

[40] N. Komin, A. C. Murza, E. Hernández-García, and R. Toral, Synchronization and entrainment of coupled circadian oscillators, Interface Focus **1**, 167 (2011).

[41] D. Gonze, S. Bernard, C. Waltermann, A. Kramer, H. Herzel, Spontaneous synchronization of coupled circadian oscillators, Biophys. J. **89**, 120 (2005).

[42] S. Bernard, D. Gonze, B. Cajavec, H. Herzel, A. Kramer, Synchronization-induced rhythmicity of circadian oscillators in the suprachiasmatic nucleus, PLoS Comput. Biol. **3**, e68 (2007).

[43] H. Kunz, P. Achermann, Simulation of circadian rhythm generation in the suprachiasmatic nucleus with locally coupled self-sustained oscillators, J. Theor. Biol. **224**, 63 (2003).

[44] C. Vasalou, E. D. Herzog, M. A. Henson, Small-world network models of intercellular coupling predict enhanced synchronization in the suprachiasmatic nucleus, J. Biol. Rhythms **24**, 243 (2009).

[45] A. B. Webb, S. R. Taylor, K. A. Thoroughman, F. J. Doyle, and E. D. Herzog, Weakly circadian cells improve resynchrony, PLoS Comput. Biol. **8**, e1002787 (2013).

[46] C. G. Gu, H. J. Yang, The circadian rhythm induced by the heterogeneous network structure of the suprachiasmatic nucleus, Chaos **26**, 053112 (2016).

[47] M. Hafner, H. Koeppl, and D. Gonze, Effect of network architecture on synchronization and entrainment properties of the circadian oscillations in the suprachiasmatic nucleus, PLoS Comput. Biol. **8**, e1002419 (2012).

[48] P. Erdős and A. Rényi, On the evolution of random graphs, Publ. Math. Debrecen **6**, 290 (1959).

[49] A. L. Barabási and R. Albert, Emergence of scaling in random networks, Science **286**, 509 (1999).

[50] See Supplemental Material at http://link.aps.org/supplemental/10.1103/PhysRevE.111.014401 for details on the effects of heterogeneous coupling on synchronization degree, period, and amplitude, and the influence of the number of neurons on synchronization degree.

[51] A. Balanov, N. Janson, D. Postnov, and O. Sosnovtseva, *Synchronization: From Simple to Complex* (Springer-Verlag, New York, 2009).

[52] S. J. Aton, C. S. Colwell, A. J. Harmar, J. Waschek, and E. D. Herzog, Vasoactive intestinal polypeptide mediates circadian rhythmicity and synchrony in mammalian clock neurons, Nat. Neurosci. **8**, 476 (2005).

[53] S. An, R. Harang, K. Meeker, D. Granados-Fuentes, C. A. Tsai, C. Mazuski, J. Kim, F. J. Doyle, L. R. Petzold, and E. D. Herzog, A neuropeptide speeds circadian entrainment by reducing intercellular synchrony, Proc. Natl. Acad. Sci. USA **110**, E4355 (2013).

[54] S. Y. Ha, S. E. Noh, and J. Park, Synchronization of Kuramoto oscillators with adaptive couplings, SIAM J. Appl. Dyn. Syst. **15**, 162 (2016).

[55] M. Manoranjani, V. R. Saiprasad, R. Gopal, D. V. Senthilkumar, and V. K. Chandrasekar, Phase transitions in an adaptive network with the global order parameter adaptation, Phys. Rev. E **108**, 044307 (2023).